
PRISM: Video Dataset Condensation with Progressive Refinement and Insertion for Sparse Motion

Jaehyun Choi Jiwan Hur Gyojin Han Jaemyung Yu Junmo Kim

Korea Advanced Institute of Science and Technology (KAIST)

{chlwogus, jiwan.hur, hangj0820, jaemyung, junmo.kim}@kaist.ac.kr

Abstract

Video dataset condensation has emerged as a critical technique for addressing the computational challenges associated with large-scale video data processing in deep learning applications. While significant progress has been made in image dataset condensation, the video domain presents unique challenges due to the complex interplay between spatial content and temporal dynamics. This paper introduces PRISM, Progressive Refinement and Insertion for Sparse Motion, for video dataset condensation, a novel approach that fundamentally reconsiders how video data should be condensed. Unlike the previous method that separates static content from dynamic motion, our method preserves the essential interdependence between these elements. Our approach progressively refines and inserts frames to fully accommodate the motion in an action while achieving better performance but less storage, considering the relation of gradients for each frame. Extensive experiments across standard video action recognition benchmarks demonstrate that PRISM outperforms existing disentangled approaches while maintaining compact representations suitable for resource-constrained environments.

1 Introduction

Machine learning research has progressed substantially through the parallel development of novel algorithmic frameworks and the growing availability of extensive training data. In the domain of computer vision, video data represents one of the richest sources of visual information, where static content elements and temporal dynamics are fundamentally intertwined, creating a comprehensive representation of our visual world. These video datasets have enabled researchers to develop models capable of understanding human actions [1, 2], tracking objects through time [3, 4], predicting future events [5], and realistic video generation [6]. As the field continues to evolve, both the quality and scale of video datasets have grown exponentially, with collections like Kinetics-700 [1], HowTo100M [7], and YouTube-8M [8] now containing millions of video clips and petabytes of data. While these expansive datasets have enabled significant progress in video understanding, they simultaneously introduce substantial computational demands for storage, preprocessing, and training. The resource requirements for working with such massive collections can limit broader participation in research with video datasets. Similarly, in the image domain, the image dataset condensation first concretized in GM [9] tackled the problem of storage and training time in image classification and achieved higher performance than the original data with condensed data that is size of only 20% of the whole dataset in DATM [10]. Building upon successes in image dataset condensation, researchers have begun exploring methods to distill the essential information from large-scale video datasets into more compact formats while preserving their effectiveness for model training.

A pioneering work by Wang et al. [11] disentangles the video into static content and dynamic motion. They employed a two-stage method, which in the first stage trains the static memory and then freezes it during the second stage, where the dynamic memory gets trained. While this decomposition may

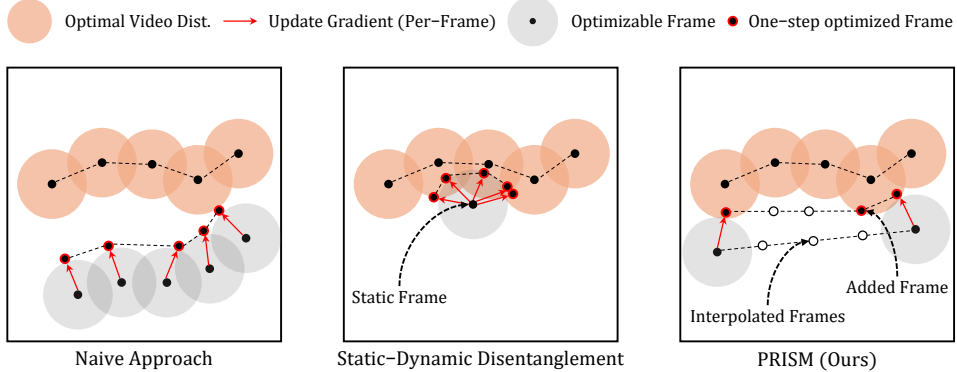


Figure 1: Visual representation of prior video dataset condensation methods and PRISM (Ours). In frame-wise matching, each frame gets updated individually, neglecting the relation between one another. Static and dynamic disentangling method [11] learn the temporal dynamics; however, it is restricted by the frozen pre-trained static image. Unlike these methods, our method learns the motion dynamics without any constraints to a single frame through a holistic approach.

offer computational advantages, it fundamentally misrepresents the intrinsic nature of real-world videos, where content and motion are not separable but rather deeply interdependent. By generating content and motion features independently, this approach neglects the crucial ways in which object positioning constrains possible motion trajectories and, conversely, how motion patterns influence the transformation of visual content throughout a sequence. For example, if a static image represents a person who is clapping, one static image could show a person with both hands touching (making the clapping sound) while another static image could show the person with hands separated. In both scenarios, the class for the video is “clapping”; however, the motion differs significantly. This demonstrates how content position within a frame inherently influences motion possibilities, and conversely, how motion patterns constrain the evolution of content.

Our method, PRISM, considers this intrinsic relationship between content and motion and is structured as illustrated in Figure 1. Rather than treating all frames equally or separating static and dynamic components as in prior work, PRISM, Progressive Refinement and Insertion for Sparse Motion, adopts a holistic optimization strategy over sparse key frames selected based on motion complexity. It begins with only two key frames per video, typically the first and last, and interpolates intermediate frames to match the expected sequence length for training. Matching losses, such as distribution matching [12] or trajectory matching [13], are applied over the interpolated sequence, but only the key frames are optimized. When interpolation fails to capture complex motion, identified by negative gradient correlation with neighboring key frames, PRISM inserts a new frame at that location. This frame is initialized by interpolation and refined jointly with the other key frames. Since this refinement and insertion process occurs independently for each class, motion-intensive actions receive more representational capacity, while simpler actions remain compact. By progressively allocating frames where needed, PRISM creates temporally coherent and memory-efficient synthetic datasets that preserve the essential dynamics of real video data. Extensive experiments on UCF-101, HMDB-51, and Something-Something-V2 demonstrate that PRISM consistently outperforms existing methods, achieving state-of-the-art results while maintaining strong content and motion fidelity.

2 Related Works

2.1 Dataset Distillation

Dataset distillation aims to synthesize a small, highly informative dataset that captures the essential characteristics of the original large-scale dataset. When models are trained on these condensed datasets, they can achieve performance comparable to training on the full dataset, but with significantly reduced computational and storage requirements. As deep learning models and datasets continue to grow in size, this field has evolved into several methodological branches.

Gradient Matching This approach ensures that synthetic data produces similar gradient updates as the original dataset. DC [9] pioneered this direction by formulating dataset distillation as a bi-level optimization problem that matches single-step gradients between original and synthetic datasets. DSA [14] enhanced this framework through differentiable Siamese augmentation, improving generalization by ensuring consistent gradients across various data transformations. IDC [15] contributed efficient parameterization strategies by storing synthetic images at lower resolutions and upsampling during training, reducing storage requirements while maintaining performance. These methods provide a direct way to ensure that synthetic data induces similar training behavior as the original dataset.

Distribution Matching These methods aim to align feature distributions between synthetic and real data, often providing more efficient alternatives to gradient-matching. DM [12] introduced a framework that aligns distributions in embedding space, significantly improving computational efficiency. CAFE [16] ensures that statistical feature properties from synthetic and real samples remain consistent across network layers, providing more comprehensive feature alignment. Distribution-matching methods typically offer better scaling properties when condensing large-scale datasets with numerous categories.

Trajectory Matching Rather than matching single-step gradients or feature distributions, these methods aim to match entire training trajectories. MTT [13] developed techniques to create condensed datasets by mimicking the training trajectories of models trained on the original dataset, significantly improving distillation efficiency. DATM [10] introduced difficulty-aligned trajectory matching to enable effective distillation without performance loss even as the synthetic dataset size changes. These approaches capture longer-range training dynamics, often resulting in better performance than single-step methods.

2.2 Video Dataset Condensation

Despite extensive research on image dataset condensation, the field of video dataset condensation remains largely unexplored, with only Wang et al. [11] making notable contributions. Their approach disentangles static content from dynamic motion by distilling videos into a single RGB static frame for content representation and a separate multi-frame single-channel component for motion. Their method follows a two-stage process: first, training the static component, then freezing it while updating only the dynamic component. Through experiments with varying numbers of condensed frames, they found that frame count does not significantly impact action recognition performance, leading to their focus on a hybrid static-dynamic representation.

Our work differs fundamentally in how it approaches the interaction between content and motion. While previous methods explicitly separate these two components by first learning a static representation and then optimizing motion as an auxiliary signal, we adopt a holistic training framework that treats the video as a fully coupled spatiotemporal structure from the beginning.

3 Method

Let $\mathcal{D} = \bigcup_{c=0}^{C-1} \mathcal{D}_c$ where $\mathcal{D}_c = \{(V_c^i, y_c^i)\}_{i=1}^{N_c}$, denote the real dataset consisting of C classes. Each video $V_c^i \in \mathbb{R}^{T \times H \times W \times 3}$ contains T frames of height H , width W and 3 color channels. The goal of video dataset condensation is to synthesize a compact synthetic dataset:

$$S = \bigcup_{c=0}^{C-1} S_c, \quad S_c = \{(S_c^j, y_c^j)\}_{j=1}^{M_c}, \quad M_c \ll N_c, \quad (1)$$

such that each condensed video S_c^j effectively captures essential spatiotemporal patterns specific to class c , while drastically reducing memory and computation costs with minimal degradation in downstream task performance.

3.1 Temporal Frame Interpolation

PRISM, Progressive Refinement and Insertion for Sparse Motion, initializes each motion sequence S_c^j using only the first and last frames of the video segment, rather than the entire sequence of T

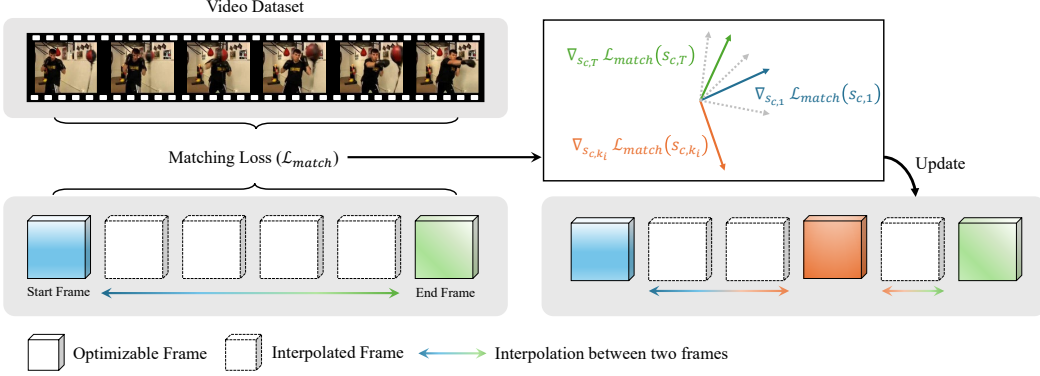


Figure 2: **Overview of PRISM.** We first initialize the key frame set as the start and the end frame. As training proceeds, we calculate the cosine similarity of the gradients for each temporally interpolated frame against all frames in the key frame set. Then, the frames that have a negative correlation with all of the current key frames are added to the key frame set and used in the subsequent training.

frames. This two-frame initialization serves as a sparse temporal anchor from which new frames are progressively inserted during training. This design is motivated by prior works in video frame interpolation, which show that simple or low-velocity motion can often be approximated by linear interpolation between the two endpoints [17, 18]. We denote this initial set of frames as:

$$S_c^j = \{s_{c,1}, s_{c,T}\}. \quad (2)$$

All intermediate frames between these key frames are populated by linear temporal interpolation to construct a full sequence of length T . Given two adjacent key frames s_{c,k_i} and $s_{c,k_{i+1}}$, the interpolated frame at time t is computed as:

$$s_{c,t} = \alpha_t s_{c,k_i} + (1 - \alpha_t) s_{c,k_{i+1}}, \quad \text{where } \alpha_t = \frac{k_{i+1} - t}{k_{i+1} - k_i}, \quad k_i < t < k_{i+1}. \quad (3)$$

Throughout the training, only the frames in S_c^j are treated as trainable parameters, while interpolated frames are held fixed.

3.2 Gradient-Guided Frame Insertion

Once the initial set $S_c^j = \{s_{c,1}, s_{c,T}\}$ is established, PRISM progressively expands this set by inserting frames that deviate from linear motion, as indicated by their gradient directions. At each training step, we consider interpolated candidate frames $s_{c,t}$ that lie between adjacent key frames s_{c,k_i} and $s_{c,k_{i+1}}$, where $k_i < t < k_{i+1}$. For each candidate frame, we compute its gradient $\nabla \mathcal{L}(s_{c,t})$ and measure its cosine similarity with the gradients of its two adjacent key frames:

$$\cos_i^t = \cos \left(\nabla_{s_{c,t}} \mathcal{L}(s_{c,t}), \nabla_{s_{c,k_i}} \mathcal{L}(s_{c,k_i}) \right), \quad \cos_{i+1}^t = \cos \left(\nabla_{s_{c,t}} \mathcal{L}(s_{c,t}), \nabla_{s_{c,k_{i+1}}} \mathcal{L}(s_{c,k_{i+1}}) \right). \quad (4)$$

If both cosine similarities are below ϵ , i.e.,

$$\cos_i^t < \epsilon \quad \text{and} \quad \cos_{i+1}^t < \epsilon, \quad (5)$$

then the candidate frame $s_{c,t}$ is considered to be the frame that is at the position of which the motion cannot be represented through linear interpolation and is inserted into the key frame set:

$$S_c^j \leftarrow S_c^j \cup \{s_{c,t}\}. \quad (6)$$

This gradient-based criterion captures non-linear transitions in appearance or motion and enables the model to refine its support set by inserting only those frames that contribute meaningful learning signals. The insertion process is repeated iteratively throughout training except for the warm-up and cool-down phases, resulting in a temporally adaptive sequence that emphasizes semantically rich regions.

Our frame insertion strategy is theoretically justified through the following lemmas.

Lemma 1 (Loss-Descent Blockage under Gradient Misalignment) *Let $s_t = \alpha s_{k_i} + (1 - \alpha) s_{k_{i+1}}$, with $0 < \alpha < 1$, be a linearly interpolated frame between two key frames s_{k_i} and $s_{k_{i+1}}$. Let the task-loss gradients be denoted as*

$$g_t = \nabla_{s_t} \mathcal{L}(s_t), \quad g_i = \nabla_{s_{k_i}} \mathcal{L}(s_{k_i}), \quad g_{i+1} = \nabla_{s_{k_{i+1}}} \mathcal{L}(s_{k_{i+1}}).$$

Suppose

$$\langle g_t, g_i \rangle < 0 \quad \text{and} \quad \langle g_t, g_{i+1} \rangle < 0.$$

Then, for every convex combination

$$v = \lambda(-g_i) + (1 - \lambda)(-g_{i+1}), \quad \lambda \in [0, 1],$$

the following inequality holds:

$$\langle g_t, v \rangle > 0.$$

Consequently, no first-order update obtained by modifying only the two endpoint frames can decrease \mathcal{L} at s_t ; the loss is stationary or strictly increasing along every such direction. Therefore, s_t must be promoted to the key-frame set and directly optimized to enable further loss minimization.

Proof. See supplementary material A. \square

3.3 Warm-Up and Cool-Down Scheduling

To ensure stable optimization and avoid the premature or unstable expansion of the key frame set, we introduce a warm-up and cool-down phase.

Warm-Up Phase During the initial warm-up period, frame insertion is disabled, and the model is trained using only the two endpoint frames in the key set $S_c^j = \{s_{c,1}, s_{c,T}\}$. This phase allows the initial frames to undergo sufficient optimization before being used as reference points for gradient-based frame comparison. Without this phase, noisy or unstable gradients from undertrained key frames may lead to unreliable insertion decisions and degrade overall sequence structure.

Cool-Down Phase In the final stage of training, frame insertion is again disabled. This prevents the inclusion of new key frames that would receive disproportionately fewer updates due to limited remaining iterations. In the context of dataset condensation, where each synthetic sample must convey maximally useful gradients, such late insertions can be detrimental. By freezing the key set in the final phase, we ensure that all selected frames are adequately trained and contribute uniformly to the optimization objective.

3.4 Optimization Objective

PRISM is integrated with Dataset Condensation via Gradient Matching (DM), where synthetic videos are optimized to match the gradient signals of real videos. The optimization is performed only over the key frame set S_c^j , which is progressively expanded during training. Interpolated frames serve solely as semantic probes and are not included in the optimization unless inserted into S_c^j .

Let θ denote the parameters of the student model, and let $\mathcal{L}_{\text{task}}$ denote the supervised loss (e.g., cross-entropy). For each class c , we define a batch of real videos $\mathcal{B}_c^{\text{real}}$ and a batch of synthetic videos $\mathcal{B}_c^{\text{syn}} = \{S_c^j\}_{j=1}^{N_c}$, where each S_c^j contains a subset of trainable frames. The optimization objective is to minimize the gradient matching loss between real and synthetic data:

$$\min_{\theta, \{S_c^j\}} \quad \sum_{c=1}^C \left\| \nabla_{\theta} \mathcal{L}_{\text{task}}(f_{\theta}(\mathcal{B}_c^{\text{syn}}), y_c) - \nabla_{\theta} \mathcal{L}_{\text{task}}(f_{\theta}(\mathcal{B}_c^{\text{real}}), y_c) \right\|_2^2. \quad (7)$$

During training, gradients are backpropagated only through the currently active key frame set S_c^j , while interpolated frames remain fixed unless inserted via the gradient-based criterion. Warm-up and cool-down phases regulate the insertion timing, ensuring stable training and sufficient updates for all selected frames.

By integrating PRISM into DM, we introduce a temporally sparse yet semantically adaptive mechanism that focuses the optimization on the most informative frames. This enables effective condensation of long video sequences into compact synthetic sets, with minimal redundancy and improved semantic coverage. The overall framework of the PRISM is illustrated in Figure 2.

Table 1: Experiment results on four video benchmarks and prior methods categorized into coresets methods, static/dynamic disentangled methods, and holistic methods. \dagger represents the author provided results. **Bold** and underline denote the best and second-best scores for each setting, respectively.

Dataset	MiniUCF			HMDB51			Kinetics-400		SSv2	
	1	5	10	1	5	10	1	5	1	5
Coreset Methods										
Random	10.9 \pm 0.7	19.6 \pm 0.4	27.8 \pm 1.1	3.3 \pm 0.1	6.8 \pm 0.7	9.8 \pm 0.4	3.0 \pm 0.2	5.5 \pm 0.2	3.1 \pm 0.1	3.6 \pm 0.1
Herding [22]	13.2 \pm 1.3	26.3 \pm 1.0	33.7 \pm 0.3	3.0 \pm 0.1	9.0 \pm 0.6	10.8 \pm 0.6	3.3 \pm 0.1	6.3 \pm 0.2	2.8 \pm 0.1	3.6 \pm 0.1
K-Center [23]	13.9 \pm 1.6	23.2 \pm 0.7	29.1 \pm 0.6	2.4 \pm 0.4	5.2 \pm 0.4	8.0 \pm 0.1	3.1 \pm 0.1	6.2 \pm 0.2	2.6 \pm 0.2	4.5 \pm 0.1
Static / Dynamic Disentangled Methods										
DM [12]	15.3 \pm 1.1	25.7 \pm 0.2	30.0 \pm 0.6	6.1 \pm 0.2	8.0 \pm 0.2	<u>12.1</u> \pm 0.4	6.3 \pm 0.0	9.1 \pm 0.9	3.6 \pm 0.0	4.1 \pm 0.0
+ Wang et al. \dagger [11]	17.5 \pm 0.1	27.2 \pm 0.4	-	6.0 \pm 0.4	8.2 \pm 0.1	-	6.3 \pm 0.2	7.0 \pm 0.1	4.0 \pm 0.1	3.8 \pm 0.1
Holistic Method										
DM + PRISM	17.9 \pm 0.3	28.0 \pm 0.1	<u>31.0</u> \pm 0.1	7.5 \pm 0.3	10.5 \pm 0.4	12.8 \pm 0.2	7.1 \pm 0.1	<u>8.1</u> \pm 0.1	<u>3.9</u> \pm 0.2	<u>4.1</u> \pm 0.1
Whole Dataset	57.8 \pm 1.1			25.4 \pm 0.2			30.3 \pm 0.1			23.0 \pm 0.3

4 Experiment

4.1 Dataset

We conduct experiments on 4 datasets: UCF101 [19] and HMDB51 [20] for small scale datasets, and Kinetics [1] and Something-Something V2 [21] for large scale datasets. UCF101 consists of 13,320 video clips of 101 action categories. Following the prior work [11], we leverage the miniaturized version of UCF101, hereinafter miniUCF, which includes the 50 most common action categories from the UCF101 dataset. HMDB51 consists of 6,849 video clips of 51 action categories. Kinetics-400 has videos of 400 human action classes and Something-Something V2 has 174 motion-centered classes.

For miniUCF and HMDB51, we sample 16 frames per video with a sampling interval of 4 and resize frames to 112×112 . For Kinetics-400 and Something-Something V2, we sample 8 frames per video and resize to 64×64 . Consistent with prior work [11], we only apply horizontal flipping with 50% probability as the sole data augmentation strategy.

4.2 Experimental Setting

For all of the experiments, we employ miniC3D, which comprises 4 Conv3D layers, as our backbone architecture following the pioneering work in video dataset condensation. Unlike DM [12], PRISM is initialized from Gaussian noise rather than initializing to a random real frame from the dataset. We report the mean of three evaluations for each experiment, measuring top-1 accuracy for miniUCF and HMDB51, and top-5 accuracy for Kinetics-400 and Something-Something V2. We compare our method against three coresets selection methods (random selection, Herding [22], and K-Center [23]), an image dataset condensation methods (DM [12]), and a video dataset condensation method (Wang et al. [11]) the first and the only video dataset condensation method. We evaluate performance under different condensation ratios, measured as Videos Per Class (VPC). Note that the VPC follows the notation of Images Per Class (IPC) in image dataset condensation and that PRISM, in most cases, will have fewer frames than 16 frames, as we are only adding frames when required. During inference, we leverage the index position for each saved vector, which is saved with the frames, with negligible memory consumption. Our experiments employ the SGD optimizer with a momentum of 0.95 for all methods. The hyperparameters, including the learning rates, are detailed in the supplementary material B.

4.3 Results

Table 1 presents the experiment results categorized as coresets methods, static and dynamic disentangled methods, and the holistic method. We categorized DM [12] as the disentangled methods as they initialize the frames from the real frames in the dataset. The results showcase that PRISM achieves state-of-the-art performance in most experimental settings. The performance increments of PRISM are smaller in the motion-centric large dataset, where only 8 frames are used for training. However,

Table 2: Storage requirements (MB) for MiniUCF and HMDB51 under different VPC settings. \dagger represents the author provided results.

Dataset	MiniUCF			HMDB51		
	VPC	1	5	10	1	5
Coreset Methods						
Random	115	586	1.15GB	115	586	1.17GB
Herding [22]	115	586	1.15GB	115	586	1.17GB
K-Center [23]	115	586	1.15GB	115	586	1.17GB
Disentangled Methods						
DM [12]	115	586	586	115	586	586
+ Wang et al. \dagger [11]	94	455	—	94	455	—
Holistic Method						
DM + PRISM	20	133	324	22	137	287
Whole Dataset	9.81GB			4.93GB		

Table 3: Results of a cross-architecture experiment on the MiniUCF dataset condensed to 1 VPC. \dagger represents the author-provided results. **Bold** denotes the best scores for each model.

Method	Evaluation Model		
	ConvNet3D	CNN+GRU	CNN+LSTM
DM	15.3 ± 1.1	9.9 ± 0.7	9.2 ± 0.3
Wang et al. \dagger	17.5 ± 0.1	12.0 ± 0.7	10.3 ± 0.2
PRISM (Ours)	17.9 ± 0.3	18.9 ± 0.8	18.2 ± 1.3

we note that we always achieve the second-best performance, if not first. Additionally, PRISM scales along with the VPC which was not the case with Wang et. al [11].

As the storage footprint of condensed data is a critical factor in dataset condensation, we report the storage requirements in Table 2. We follow the same calculation procedure as prior work [11], treating each sample as a `float32` tensor. For PRISM, the reported storage corresponds to the total number of frames retained after the condensation process completes for each VPC setting. We ignore the negligible overhead from storing frame indices (less than 0.000016 MB per index).

Unlike previous methods that begin with a fixed number of frames (e.g., 16), PRISM starts with only 2 key frames per video and progressively inserts additional frames only when the cosine similarity between gradients is negative. This selective strategy results in a significantly lower storage footprint—up to a 75% reduction compared to prior approaches—while achieving superior performance. Moreover, since PRISM adds frames adaptively rather than proportionally to the number of VPCs, its storage does not grow linearly with VPC. This behavior is clearly visible in the miniUCF results, where storage grows much more slowly than would be expected under proportional expansion. Such efficiency makes PRISM especially advantageous when users wish to scale up performance under higher VPC budgets without incurring prohibitive storage costs.

5 Ablation

Cross-Architecture As dataset condensation aims to perform well not only on the training model but also on other architectures, we validate our approach’s robustness through Table 3. The experimental results demonstrate that PRISM not only achieves state-of-the-art performance compared to prior methods but also maintains robust performance across different architectures. Notably, while DM and Wang et al. [11] show significant performance drops when evaluated on CNN+GRU, our method maintains consistent performance with only minimal degradation. This strong cross-architecture generalization underscores the strength of our holistic design, which preserves the intrinsic coupling between content and motion—an essential property of video data often overlooked by prior methods.

Effect of Number of Initial Key Frames Table 4 presents results when varying the number of initial key frames for the condensation process. We observe a consistent decrease in performance as

Table 4: Results by varying the number of initial representative frames of PRISM. **Bold** denotes the best scores for each dataset.

Dataset	Number of Initial Key Frames				
	2	3	4	6	8
MiniUCF	17.9 \pm 0.3	16.4 \pm 0.5	15.9 \pm 0.3	15.0 \pm 0.2	14.8 \pm 0.2
HMDB51	7.5 \pm 0.3	6.4 \pm 0.2	6.0 \pm 0.4	5.2 \pm 0.4	4.9 \pm 0.2

Table 5: Ablation study results for (A) with and without insertion, (B) frame selection strategy, (C) similarity metric, and (D) training phase scheduling (warm-up and cool-down).

(A)			(B)		
Dataset	w/ Insertion	w/o Insertion	Dataset	Negative Grad.	Random Pos.
MiniUCF	17.9 \pm 0.3	15.8 \pm 1.2	MiniUCF	17.9 \pm 0.3	16.8 \pm 0.4
HMDB51	7.5 \pm 0.3	6.1 \pm 0.3	HMDB51	7.5 \pm 0.3	6.8 \pm 0.2
(C)			(D)		
Dataset	Cosine Sim.	L2 Distance	Dataset	w/o Warm-Up	w/o Cool-Down
MiniUCF	17.9 \pm 0.3	15.7 \pm 0.7	MiniUCF	16.1 \pm 0.8	16.9 \pm 1.3
HMDB51	7.5 \pm 0.3	6.0 \pm 0.6	HMDB51	6.8 \pm 1.2	6.3 \pm 0.3

the number of key frames increases. This trend suggests that while more initial frames may cover more content, they also introduce more redundancy and dilute the discriminative capacity of the condensed set as well as optimization complexity, making updates more difficult. This leads to a less focused optimization signal, especially in the early stages of training. The result highlights the importance of a sparse but minimally selected number of frame initialization rather than simply increasing the number of input frames.

Without Frame Insertion One of PRISM’s core contributions is the progressive insertion of frames based on gradient cues. To isolate the effect of this component, we perform an ablation where only two key frames (the first and last) are optimized throughout training. Temporal interpolation is still applied between these endpoints, but no additional key frames are inserted. As shown in Table 5 (A), removing this progressive insertion leads to a substantial performance drop, confirming that our insertion strategy is critical for capturing complex motion and structure. Nevertheless, this reduced variant still outperforms several existing baselines using real images, despite being initialized from Gaussian noise. This suggests that even a minimal version of our method can serve as a competitive and meaningful baseline for video dataset condensation.

Frame Selection Strategy We evaluate the effectiveness of our gradient-based frame selection by comparing it against a random selection baseline. Both methods operate under identical conditions: a new frame is inserted whenever a negative cosine similarity is detected between gradients. However, while PRISM selects the frame with the most negative cosine similarity, the baseline instead randomly selects one from the candidate pool, including the negatively correlated one. This setup ensures that the two methods differ only in how the new frame is selected, not in how often frames are added or when. As shown in Table 5 (B), replacing our targeted frame selection with random addition results in substantial performance drops across both datasets. This confirms that gradient correlation is not just a useful signal but a decisive factor in identifying semantically meaningful frames that enhance the condensation process.

Cosine Similarity vs. L2 Distance PRISM uses cosine similarity to identify frames whose gradients are directionally misaligned with those of existing key frames, signaling potential discontinuities in motion or content. This angle-based criterion is particularly effective for capturing semantic transitions, as it not only measures the degree of difference but also the directional disagreement between gradients. To test whether cosine similarity is truly essential, we compare it against a distance-based alternative using the L2 norm. However, unlike cosine similarity, which has a well-defined geometric interpretation (e.g., zero for orthogonal gradients), L2 distance lacks a natural threshold. To make the comparison meaningful, we calibrated the L2 threshold to 0.141, which corresponds to 10% of the unit vector distance implied by a 90-degree angular separation in cosine

space. As shown in Table 5 (C), cosine similarity significantly outperforms L2 distance across both HMDB51 and miniUCF. These results confirm that directional disagreement, rather than magnitude alone, is a more reliable indicator of frame-level semantic variation, justifying our use of cosine similarity for frame insertion in PRISM.

Effect of Warm-Up and Cool-Down Phases To stabilize training and prevent premature or noisy frame insertions, PRISM incorporates both a warm-up and a cool-down phase. The warm-up phase delays the start of frame insertion to allow gradients to stabilize around the initial key frames. The cool-down phase, on the other hand, suspends further insertions once the condensation process nears convergence, preventing overfitting or unnecessary growth in the synthetic video set. To evaluate the necessity of each phase, we conduct ablations where either the warm-up or cool-down phase is removed. As shown in Table 5 (D), removing either phase degrades performance, with the absence of the cool-down phase leading to over-insertion and noisy representation, and the absence of the warm-up phase causing unstable optimization due to early gradient noise. These findings confirm that both the warm-up and cool-down stages are integral to PRISM’s temporal curriculum, ensuring effective and stable condensation dynamics throughout training. All qualitative results can be found in the supplementary material D.

Optical Flow Result To qualitatively assess whether the frames selected through our gradient-based criterion capture meaningful temporal dynamics, we visualize the class-wise mean optical flow on the miniUCF dataset. Figure 3 compares the average optical flow of real videos (top) with that of our condensed data generated using only negatively correlated frames ($IPC = 5$, bottom) for the class *Soccer Penalty*. Despite the aggressive frame reduction, our method produces motion patterns that closely resemble those of the real videos. This result implies that selecting frames based on gradient misalignment is not only computationally principled but also semantically grounded—our approach reliably detects the frames responsible for key motion events, even without any supervision. More qualitative evaluations are provided in the supplementary material C.

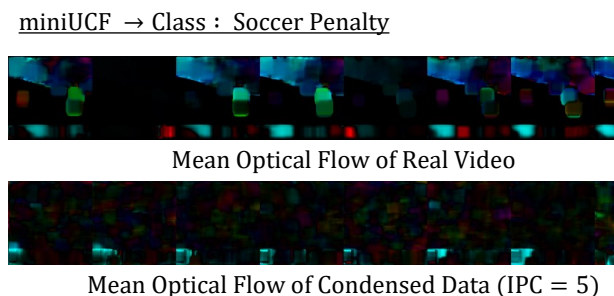


Figure 3: Optical-flow comparison for the Soccer Penalty class on miniUCF.

Limitations While PRISM enables efficient and adaptive frame selection under typical spatiotemporal conditions, it may encounter limitations under two challenging regimes. First, in videos with extremely fast or abrupt motion, the linear interpolation between key frames may fail to approximate intermediate dynamics, especially when the number of frames inserted is insufficient. As PRISM relies on gradient-based cues to detect non-linearity, such rapid transitions may not always manifest as cleanly separable cosine misalignment, particularly early in training when gradients are noisy. Second, when applied to very long video sequences, the initial frame optimization from Gaussian noise may become unstable. This resembles difficulties observed in long-range video generation, where spatiotemporal consistency becomes harder to preserve over extended durations. Although our warm-up and cool-down phases mitigate some of these effects, scaling PRISM to extreme motion speeds or extended temporal horizons may require additional stabilization strategies.

6 Conclusion

This paper introduced Progressive Refinement and Insertion for Sparse Motion (PRISM), a novel approach that preserves the interdependence between content and motion in videos. Unlike previous methods that artificially separate these elements, our holistic approach begins with minimal representation and strategically adds frames where gradient correlation indicates complex motion patterns. Experiments across multiple benchmarks demonstrate that PRISM outperforms existing methods while reducing storage requirements by up to 70%. Our method maintains better cross-architecture generalization and adapts the number of frames based on class-specific motion complexity.

References

- [1] J. Carreira and A. Zisserman, “Quo vadis, action recognition? a new model and the kinetics dataset,” in *proceedings of the IEEE Conference on Computer Vision and Pattern Recognition*, 2017, pp. 6299–6308.
- [2] L. Wang, Y. Xiong, Z. Wang, Y. Qiao, D. Lin, X. Tang, and L. Van Gool, “Temporal segment networks: Towards good practices for deep action recognition,” in *European conference on computer vision*. Springer, 2016, pp. 20–36.
- [3] L. Bertinetto, J. Valmadre, J. F. Henriques, A. Vedaldi, and P. H. Torr, “Fully-convolutional siamese networks for object tracking,” in *Computer vision–ECCV 2016 workshops: Amsterdam, the Netherlands, October 8–10 and 15–16, 2016, proceedings, part II 14*. Springer, 2016, pp. 850–865.
- [4] B. Li, J. Yan, W. Wu, Z. Zhu, and X. Hu, “High performance visual tracking with siamese region proposal network,” in *Proceedings of the IEEE conference on computer vision and pattern recognition*, 2018, pp. 8971–8980.
- [5] Y. A. Farha and J. Gall, “Ms-tcn: Multi-stage temporal convolutional network for action segmentation,” in *Proceedings of the IEEE/CVF conference on computer vision and pattern recognition*, 2019, pp. 3575–3584.
- [6] S. Tulyakov, M.-Y. Liu, X. Yang, and J. Kautz, “Mocogan: Decomposing motion and content for video generation,” in *Proceedings of the IEEE conference on computer vision and pattern recognition*, 2018, pp. 1526–1535.
- [7] A. Miech, D. Zhukov, J.-B. Alayrac, M. Tapaswi, I. Laptev, and J. Sivic, “Howto100m: Learning a text-video embedding by watching hundred million narrated video clips,” in *Proceedings of the IEEE/CVF international conference on computer vision*, 2019, pp. 2630–2640.
- [8] S. Abu-El-Haija, N. Kothari, J. Lee, P. Natsev, G. Toderici, B. Varadarajan, and S. Vijayanarasimhan, “Youtube-8m: A large-scale video classification benchmark,” *arXiv preprint arXiv:1609.08675*, 2016.
- [9] B. Zhao, K. R. Mopuri, and H. Bilen, “Dataset condensation with gradient matching,” *arXiv preprint arXiv:2006.05929*, 2020.
- [10] Z. Guo, K. Wang, G. Cazenavette, H. Li, K. Zhang, and Y. You, “Towards lossless dataset distillation via difficulty-aligned trajectory matching,” *arXiv preprint arXiv:2310.05773*, 2023.
- [11] Z. Wang, Y. Xu, C. Lu, and Y.-L. Li, “Dancing with still images: video distillation via static-dynamic disentanglement,” in *Proceedings of the IEEE/CVF Conference on Computer Vision and Pattern Recognition*, 2024, pp. 6296–6304.
- [12] B. Zhao and H. Bilen, “Dataset condensation with distribution matching,” in *Proceedings of the IEEE/CVF Winter Conference on Applications of Computer Vision*, 2023, pp. 6514–6523.
- [13] G. Cazenavette, T. Wang, A. Torralba, A. A. Efros, and J.-Y. Zhu, “Dataset distillation by matching training trajectories,” in *Proceedings of the IEEE/CVF Conference on Computer Vision and Pattern Recognition*, 2022, pp. 4750–4759.
- [14] B. Zhao and H. Bilen, “Dataset condensation with differentiable siamese augmentation,” in *International Conference on Machine Learning*. PMLR, 2021, pp. 12 674–12 685.
- [15] J.-H. Kim, J. Kim, S. J. Oh, S. Yun, H. Song, J. Jeong, J.-W. Ha, and H. O. Song, “Dataset condensation via efficient synthetic-data parameterization,” in *International Conference on Machine Learning*. PMLR, 2022, pp. 11 102–11 118.
- [16] K. Wang, B. Zhao, X. Peng, Z. Zhu, S. Yang, S. Wang, G. Huang, H. Bilen, X. Wang, and Y. You, “Cafe: Learning to condense dataset by aligning features,” in *Proceedings of the IEEE/CVF Conference on Computer Vision and Pattern Recognition*, 2022, pp. 12 196–12 205.
- [17] S. Niklaus, L. Mai, and F. Liu, “Video frame interpolation via adaptive convolution,” in *Proceedings of the IEEE conference on computer vision and pattern recognition*, 2017, pp. 670–679.
- [18] Z. Liu, R. A. Yeh, X. Tang, Y. Liu, and A. Agarwala, “Video frame synthesis using deep voxel flow,” in *Proceedings of the IEEE international conference on computer vision*, 2017, pp. 4463–4471.
- [19] K. Soomro, A. R. Zamir, and M. Shah, “Ucf101: A dataset of 101 human actions classes from videos in the wild,” *arXiv preprint arXiv:1212.0402*, 2012.

- [20] H. Kuehne, H. Jhuang, E. Garrote, T. Poggio, and T. Serre, "Hmdb: a large video database for human motion recognition," in *2011 International conference on computer vision*. IEEE, 2011, pp. 2556–2563.
- [21] R. Goyal, S. Ebrahimi Kahou, V. Michalski, J. Materzynska, S. Westphal, H. Kim, V. Haenel, I. Fruend, P. Yianilos, M. Mueller-Freitag *et al.*, "The" something something" video database for learning and evaluating visual common sense," in *Proceedings of the IEEE international conference on computer vision*, 2017, pp. 5842–5850.
- [22] M. Welling, "Herding dynamical weights to learn," in *Proceedings of the 26th annual international conference on machine learning*, 2009, pp. 1121–1128.
- [23] O. Sener and S. Savarese, "Active learning for convolutional neural networks: A core-set approach," *arXiv preprint arXiv:1708.00489*, 2017.

A Proof of Lemma 1

Lemma 1 (Loss-Descent Blockage under Gradient Misalignment) *Let $s_t = \alpha s_{k_i} + (1 - \alpha) s_{k_{i+1}}$, with $0 < \alpha < 1$, be a linearly interpolated frame between two key frames s_{k_i} and $s_{k_{i+1}}$. Let the task-loss gradients be denoted as*

$$g_t = \nabla_{s_t} \mathcal{L}(s_t), \quad g_i = \nabla_{s_{k_i}} \mathcal{L}(s_{k_i}), \quad g_{i+1} = \nabla_{s_{k_{i+1}}} \mathcal{L}(s_{k_{i+1}}).$$

Suppose

$$\langle g_t, g_i \rangle < 0 \quad \text{and} \quad \langle g_t, g_{i+1} \rangle < 0.$$

Then, for every convex combination

$$v = \lambda(-g_i) + (1 - \lambda)(-g_{i+1}), \quad \lambda \in [0, 1],$$

the following inequality holds:

$$\langle g_t, v \rangle > 0.$$

Consequently, no first-order update obtained by modifying only the two endpoint frames can decrease \mathcal{L} at s_t ; the loss is stationary or strictly increasing along every such direction. Therefore, s_t must be promoted to the key frame set and directly optimized to enable further loss minimization.

Proof. By the bilinearity of the inner product,

$$\langle g_t, v \rangle = \lambda \langle g_t, -g_i \rangle + (1 - \lambda) \langle g_t, -g_{i+1} \rangle.$$

Applying the assumption $\langle g_t, g_i \rangle < 0$, we obtain

$$\langle g_t, -g_i \rangle = -\langle g_t, g_i \rangle > 0,$$

and similarly,

$$\langle g_t, -g_{i+1} \rangle = -\langle g_t, g_{i+1} \rangle > 0.$$

Therefore,

$$\langle g_t, v \rangle = \lambda \cdot \langle g_t, -g_i \rangle + (1 - \lambda) \cdot \langle g_t, -g_{i+1} \rangle > 0.$$

This shows that the directional derivative of \mathcal{L} at s_t along any direction v formed by adjusting only the endpoints is positive:

$$D_v \mathcal{L}(s_t) = \langle \nabla \mathcal{L}(s_t), v \rangle > 0.$$

Thus, no first-order update along such directions can reduce the loss at s_t , and $\mathcal{L}(s)$ is strictly increasing along all directions spanned by $-g_i$ and $-g_{i+1}$. It follows that further loss minimization requires directly optimizing s_t as a key frame. \square

B Hyperparameter

In Table A, we show the learning rate and batch size under each dataset and IPC. The ϵ is set to 0 for all experiments throughout the manuscript. The warm-up and cool-down phases are processed for 20% of the whole iteration each. In other words, if the condensation process is set to 100 iterations, the warm-up phase takes up the first 20 iterations and the cool-down phase takes up the last 20 iterations, leaving 80 iterations for the progressive refinement and insertion of frames. We follow the setting from the prior method [11] for evaluation and cross-architecture evaluation.

Table A: Hyperparameters for PRISM under different datasets and IPC.

Method	Dataset	Train			Evaluation	
		IPC	LR	Batch Real	Epoch	LR
DM	MiniUCF	1	1	64		
		5	25	64		
		10	50	64		
	HMDB51	1	0.7	64		
		5	25	64	500	$1e^{-2}$
		10	75	64		
	Kinetics-400	1	1	64		
		5	50	128		
	SSv2	1	3	64		
		5	30	128		

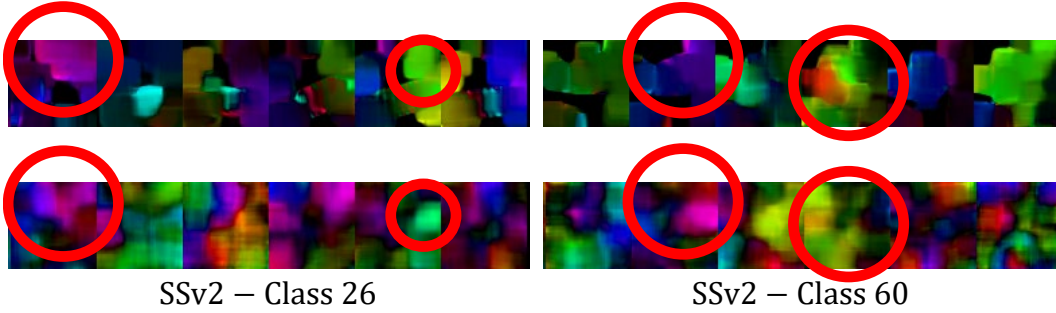


Figure 4: Extra optical flow results on SSv2 under 1 VPC setting. The red circle shows where the optical flow matches the most between the condensed video and the real video.

C Optical Flow Analysis

To further assess the temporal fidelity of our condensation framework, we visualize the optical flow fields of both real and condensed videos. Optical flow represents the pixel-wise motion between consecutive frames and serves as a direct indicator of whether the synthesized frames preserve realistic temporal dynamics. In our visualizations in the supplementary and also in the main manuscript, we use a standard HSV-based color encoding, where the hue (i.e., the color itself) corresponds to the direction of motion—such as rightward appearing reddish, leftward bluish, and upward greenish—while the saturation and brightness encode the magnitude of motion, with brighter and more saturated regions indicating stronger or faster motion. Regions with little to no motion appear desaturated or grayish.

Despite beginning from Gaussian noise and adding frames along training, the optical flow results show that PRISM is capable of progressively aligning the synthesized motion with that of the real video. As shown in Figure 5, the red circles highlight regions where the direction and magnitude of the condensed optical flow closely resemble those of the original video. This further supports the observation that PRISM can synthesize coherent motion dynamics from sparsely supervised temporal supervision.

Nevertheless, some failure modes are also apparent in these optical flow visualizations. In cases where the first and last frames contain minimal or no motion, the model struggles and generates meaningless or abrupt motion during warm-up phase. Moreover, in action classes that involve fast or abrupt motions, the resulting flow fields from the condensed video occasionally lack directional consistency and show spatial noise, indicating poor alignment. These limitations appear to be exacerbated by the use of Gaussian noise initialization, which may hinder the model’s ability to focus solely on the informative motion patterns at early training stages.

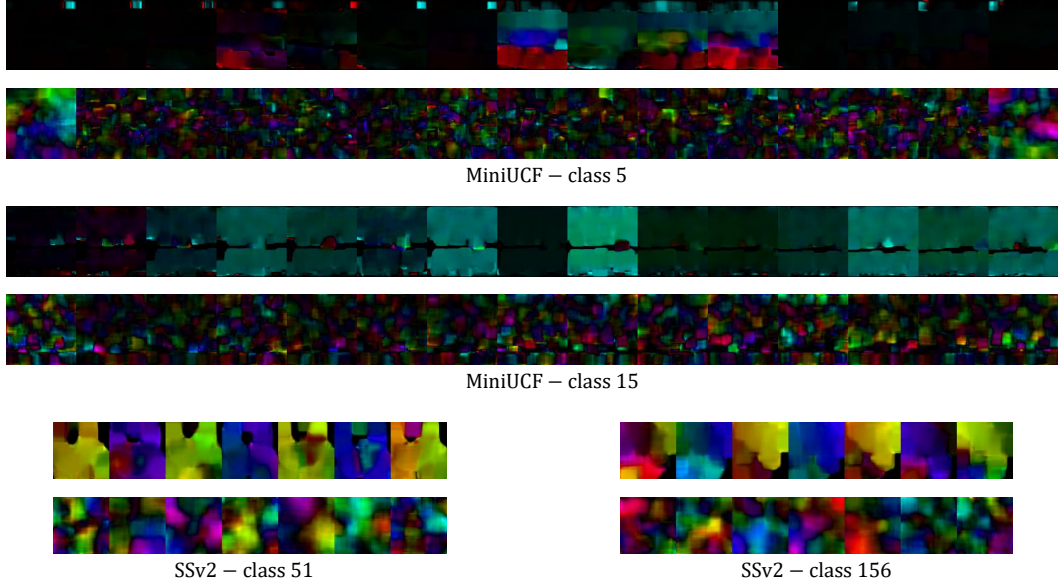


Figure 5: Analysis on when PRISM fails.

D Qualitative Results

We visualize the condensed videos on HMDB51 and MiniUCF under the 1 VPC setting for maximal clarity. The visualized frames in Figure 6 and Figure 7 correspond to those retained after the condensation process, where the noise images are placeholders which does not get stored along with condensed data.

Red rectangles highlight the negative effect when the warm-up phase is omitted. As consistently observed across both datasets, removing the warm-up leads to excessive frame selection, resulting in redundant and less informative synthetic frames while consuming more memory.

Blue rectangles indicate frames produced when the cool-down phase is omitted. Although overall results appear more stable than in the warm-up-removed case, we observe that some frames are added during the final few iterations of condensation. These late-added frames often lack sufficient training, reducing their utility for action recognition by being not fully trained.



Figure 6: Visualization of PRISM, PRISM without warm-up, and PRISM without cool-down on HMDB51 under 1 VPC. Red rectangles highlight the negative effects of omitting the warm-up phase, while blue rectangles indicate frames that may be under-trained due to the absence of a cool-down phase.



Figure 7: Visualization of PRISM, PRISM without warm-up, and PRISM without cool-down on MiniUCF under 1 VPC. Red rectangles highlight the negative effects of omitting the warm-up phase, while blue rectangles indicate frames that may be under-trained due to the absence of a cool-down phase.